

# Resolving the Degeneracy in Single Higgs Production with Higgs Pair Production

Qing-Hong Cao,<sup>1, 2, 3,\*</sup> Bin Yan,<sup>1, †</sup> Dong-Ming Zhang,<sup>1, ‡</sup> and Hao Zhang<sup>4, §</sup>

<sup>1</sup>*Department of Physics and State Key Laboratory of Nuclear Physics and Technology, Peking University, Beijing 100871, China*

<sup>2</sup>*Collaborative Innovation Center of Quantum Matter, Beijing, China*

<sup>3</sup>*Center for High Energy Physics, Peking University, Beijing 100871, China*

<sup>4</sup>*Department of Physics, University of California, Santa Barbara, CA 93106, USA*

The Higgs boson production can be affected by several anomalous couplings, e.g.  $c_t$  and  $c_g$  anomalous couplings. Precise measurement of  $gg \rightarrow h$  production yields two degenerate parameter spaces of  $c_t$  and  $c_g$ ; one parameter space exhibits the SM limit while the other does not. Such a degeneracy could be resolved by Higgs boson pair production. In this work we adapt the strategy suggested by the ATLAS collaboration to explore the potential of distinguishing the degeneracy at the 14 TeV LHC. If the  $c_t$  anomalous coupling is induced only by the operator  $H^\dagger H \bar{Q}_L \tilde{H} t_R$ , then the non-SM-like band could be excluded with an integrated luminosity of  $\sim 235 \text{ fb}^{-1}$ . Making use of the fact that the Higgs boson pair is mainly produced through an  $s$ -wave scattering, we propose an analytical function to describe the fraction of signal events surviving a series of experimental cuts for a given invariant mass of Higgs boson pair. The function is model independent and can be applied to estimate the discovery potential of various NP models.

**Introduction:** In the establishment of the Standard Model (SM), thousands of experiments have been performed to measure model parameters and check the consistency of the theory. In the same spirit, it is critical to measure all the properties of the recently discovered Higgs boson as precisely as possible to test the SM and probe New Physics (NP) beyond the SM. The Higgs couplings have been constrained at the LHC Run-1 [1, 2]. In the SM the Higgs boson is predominantly produced through the gluon fusion process which can be affected by either  $h\bar{t}t$  or  $hgg$  anomalous couplings. The anomalous couplings are described by the effective Lagrangian  $\mathcal{L} = -\frac{m_t}{v} c_t h\bar{t}t + \frac{\alpha_s}{12\pi v} c_g h G_{\mu\nu}^a G_a^{\mu\nu}$ . Figure 1 displays the parameter space of  $c_t$  and  $c_g$  allowed by the measurement. Two degenerate parameter spaces arise from the interference of  $c_t$  and  $c_g$  contributions. For example, in the heavy top-quark limit,

$$\sigma_{\text{NP}}(gg \rightarrow h) \simeq \sigma_{\text{SM}}(gg \rightarrow h) \times |c_g + c_t|^2. \quad (1)$$

The upper band in Fig. 1 corresponds to  $c_t + c_g \sim +1$ , which has a SM limit of  $c_t \rightarrow 1$  and  $c_g \rightarrow 0$ . We name it as “SM-like” band. The lower band corresponds to  $c_t + c_g \sim -1$ , which does not exhibit the SM limit. In the lower band the NP contributions should cancel the SM contribution out and leads to a residual contribution of minus SM value. Though often ignored, it is possible in principle<sup>1</sup>. We name the lower band as the “faked-no-new-physics” (FNNP) band since further improvement in

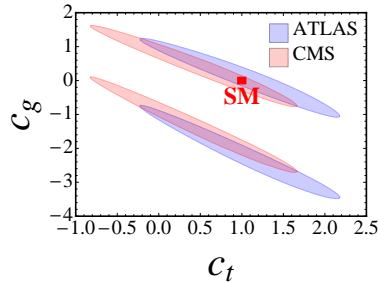


FIG. 1. The bounds at 95% confidence level (C.L.) in the plane of  $c_t$  and  $c_g$  from the ATLAS [1] and CMS [2] collaborations. The red box denotes the SM ( $c_t = 1, c_g = 0$ ).

the measurement of single Higgs-boson productions cannot distinguish it from the upper SM-like band. The Higgs boson pair production  $gg \rightarrow hh$ , which is highly correlated with the  $gg \rightarrow h$  process, can be used to discriminate the SM-like and FNNP bands [3–5]. In this work, we focus our attentions on the ATLAS constraints and explore the potential of the 14 TeV LHC to exclude the FNNP band in the Higgs boson pair production.

**Higgs boson pair production:** The Higgs boson pair production is usually considered as the best channel to measure the Higgs trilinear coupling in the SM [6–23]. It is also sensitive to various NP models [24–65]. In this work we adapt the effective Lagrangian approach to describe the unknown NP effects. After the electroweak symmetry breaking the effective Lagrangian related to the double Higgs production is [4, 66–71]

$$\begin{aligned} \mathcal{L}_h = & -\frac{m_h^2}{2v} c_3 h^3 - \frac{m_t}{v} c_t \bar{t}_L t_R h - \frac{m_t}{v^2} c_{2h} \bar{t}_L t_R h^2 \\ & + \frac{\alpha_s c_g}{12\pi v} h G_{\mu\nu}^a G_a^{\mu\nu} + \frac{\alpha_s c_g}{24\pi v^2} h^2 G_{\mu\nu}^a G_a^{\mu\nu} + \text{h.c.} , \quad (2) \end{aligned}$$

where  $v = 246$  GeV is the vacuum expectation value,  $\alpha_s = g_s^2/4\pi$  with  $g_s$  the strong coupling strength,  $m_t$  is

<sup>1</sup> For example, additional colored  $SU(2)_L$  singlet scalars ( $S_i$ ) could generate a large negative  $c_g$  in the FNNP band. The scalar  $S_i$ ’s interact with the SM Higgs boson via  $-k_i S_i^* S_i H^\dagger H$  with  $H$  the SM Higgs boson doublet. Integrating out heavy  $S_i$ ’s inside the  $gg \rightarrow h$  triangle loop yields  $c_g \sim \sum_i T(S_i) k_i v^2 / (4m_{S_i}^2)$  where  $T(S_i)$  is the Dynkin index of  $S_i$  for the corresponding representation under  $SU(3)_C$ .

the top-quark mass and  $m_h$  is the Higgs boson mass. In the SM,  $c_3 = c_t = 1$  and  $c_{2h} = c_g = 0$ . The squared amplitude of  $gg \rightarrow hh$  averaging over the gluon polarizations and colors is [63]

$$\overline{|\mathcal{M}|^2} = \frac{\alpha_s^2 \hat{s}^2}{256\pi^2 v^4} \left[ \left| \frac{3m_h^2}{\hat{s} - m_h^2} c_3 \left( c_t F_\Delta + \frac{2}{3} c_g \right) + 2c_{2h} F_\Delta + c_t^2 F_\square + \frac{2}{3} c_g \right|^2 + |c_t^2 G_\square|^2 \right], \quad (3)$$

where  $F_\Delta \equiv F_\Delta(\hat{s}, \hat{t}, m_h^2, m_t^2)$ ,  $F_\square \equiv F_\square(\hat{s}, \hat{t}, m_h^2, m_t^2)$  and  $G_\square \equiv G_\square(\hat{s}, \hat{t}, m_h^2, m_t^2)$  are the form factors [24] with  $\hat{s}$  and  $\hat{t}$  the canonical Mandelstam variables.  $G_\square$  corresponds to the  $d$ -wave component which is negligible [46].

In order to compare  $\sigma(gg \rightarrow hh)$  with the SM prediction, we define a ratio  $R_{hh}$  as

$$R_{hh} = \frac{\sigma(gg \rightarrow hh)}{\sigma^{\text{SM}}(gg \rightarrow hh)}. \quad (4)$$

Figure 2 displays the contours of  $R_{hh} = 1, 5$  and 10 in the plane of anomalous couplings for four benchmark choices:

- (a)  $c_3 = 1, c_{2h} = 0$ ;
- (b)  $c_3 = 1, c_{2h} = 3(c_t - 1)/2$ ;
- (c)  $c_3 = c_t = 1$ ;
- (d)  $c_t = 1, c_{2h} = 0$ .

(5)

In the case (b) we assume that both  $c_t$  and  $c_{2h}$  anomalous couplings are induced by the operator  $H^\dagger H \bar{Q}_L \tilde{H} t_R$  and thus exhibit the relation. The production cross section of the Higgs boson pair is enhanced in the FNNP band in all the four choices:

- (a)  $1.44 < R_{hh} < 92.89$ ;
- (b)  $11.12 < R_{hh} < 46.58$ ;
- (c)  $3.46 < R_{hh} < 88.86$ ;
- (d)  $9.11 < R_{hh} < 12.64$ .

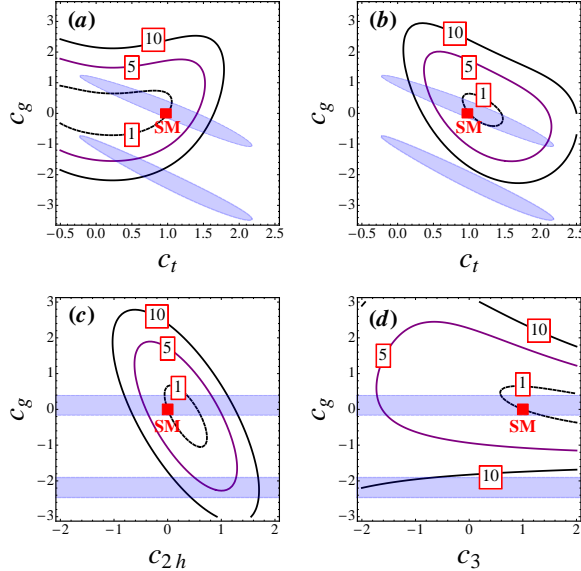


FIG. 2. The contours of  $R_{hh} = 1, 5$  and 10 in the plane of anomalous couplings at the 14 TeV LHC. The figure indices correspond to the benchmark choices of anomalous couplings in Eq. 5.

**Collider simulation:** Next we perform a detailed Monte Carlo simulation to estimate the needed integrated luminosity for probing or excluding the FNNP band at the 14 TeV LHC. As a concrete example, we examine the  $hh \rightarrow b\bar{b}\gamma\gamma$  channel, which has been studied by the ATLAS collaboration [72]. MadGraph5 [73] is used to generate the signal events at the parton-level with CT14 [74] and MSTW2008 [75] parton distribution function (PDF). Following the ATLAS study [72], the signal events must contain two  $b$ -tagged jets and two isolated photons which satisfy the kinematic cuts as follows:

$$\begin{aligned} p_T^{\text{leading } b} &> 40 \text{ GeV}, \quad p_T^b > 25 \text{ GeV}, \quad |\eta^b| < 2.5, \\ p_T^\gamma &> 30 \text{ GeV}, \quad |\eta^\gamma| < 1.37 \text{ or } 1.52 < |\eta^\gamma| < 2.37, \\ \Delta R_0 &< \Delta R_{b\bar{b},\gamma\gamma} < 2.0, \quad \Delta R_{b\gamma} > \Delta R_0, \quad \Delta R_0 = 0.4, \\ 100 \text{ GeV} &< m_{b\bar{b}} < 150 \text{ GeV}, \quad p_T^{b\bar{b}} > 110 \text{ GeV}, \\ 123 \text{ GeV} &< m_{\gamma\gamma} < 128 \text{ GeV}, \quad p_T^{\gamma\gamma} > 110 \text{ GeV}. \end{aligned}$$

In order to mimic the imperfect detector effects, we smear the final state parton momenta by a Gaussian distribution as suggested in Ref. [76]. The  $b$  identification strongly depends on  $p_T^b$  and  $\eta^b$ . We fit the  $b$ -tagging efficiency given in the ATLAS Technique Report [77] and obtain the following function of the  $b$ -tagging efficiency:

$$\epsilon_b(p_T, \eta) = 0.135 \tanh\left(\frac{p_T + 50}{75}\right) \tanh\left(\frac{450}{p_T + 80}\right) \times [3 + e^{-\left(|\eta| - \sqrt{p_T/1000}\right)^2/1.6}] e^{-|\eta|^3 p_T/1000}, \quad (6)$$

where  $p_T$  is in the unit of GeV. Figure 4 displays our  $b$ -tagging efficiency as a function of  $p_T^b$  and  $\eta^b$ , which agrees well with the ATLAS study.

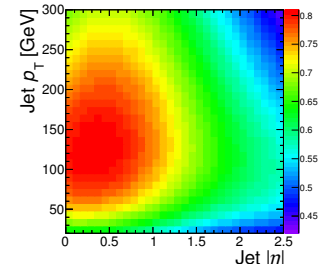


FIG. 3. The  $b$ -tagging efficiency as a function of  $p_T^b$  and  $\eta^b$ .

The photon energy resolution and identification are crucial to trigger and reconstruct the signal events. In the simulation we adapt the photon energy resolution and identification efficiency given by the ATLAS collaboration [77]. The photon energy resolution is given as follows:

$$\begin{aligned} \sigma(\text{GeV}) &= 0.3 \oplus 0.10 \times \sqrt{E(\text{GeV})} \oplus 0.010 \times E(\text{GeV}), \\ &\quad \text{for } |\eta| < 1.37, \\ \sigma(\text{GeV}) &= 0.3 \oplus 0.15 \times \sqrt{E(\text{GeV})} \oplus 0.015 \times E(\text{GeV}), \\ &\quad \text{for } 1.52 < |\eta| < 2.37. \end{aligned} \quad (7)$$

The identification efficiency, which is sensitive to  $p_T^\gamma$ , is given by

$$\epsilon_\gamma(p_T) = 0.76 - 1.98 \exp\left(-\frac{p_T}{16.1 \text{GeV}}\right), \quad (8)$$

Note that the identification rate is less than 80% even for an energetic photon.

The key of collider simulation is to know the so-called cut efficiency, i.e. the fraction of signal events passing the kinematic cuts. To understand the cut efficiencies of different values of anomalous couplings, one has to repeat the collider simulation which include all the kinematic cuts, imperfect detector resolutions and particle identifications, etc. However, it is very time consuming in practice. Inspired by the scalar feature of Higgs boson, we propose an analytical function to describe the fraction of signal events passing through the kinematic cuts. The function depends upon the invariant mass of the Higgs boson pair ( $m_{hh}$ ) and is not sensitive to those anomalous couplings or specific NP model. The advantage of our method is that the cut efficiency of the  $hh$  signal events can be easily obtained from the convolution of the differential cross section of  $d\sigma/dm_{hh}$  and the cut efficiency function. The method is explained below.

The scattering of  $gg \rightarrow hh$  is dominated by the  $s$ -wave contribution. Owing to the scalar feature of the Higgs boson, there is no spin correlations among the initial state and final state particles. Therefore, the  $p_T$  and  $\eta$  distributions of the  $b$ -jets and photons depend mainly upon  $m_{hh}$ . The differential cross section of the  $gg \rightarrow hh$  process before any cut is

$$\begin{aligned} \frac{d\sigma}{dm_{hh}} &= \frac{m_{hh}}{S^2} \mathcal{H}(m_{hh}, \mu_r) \int_{m_{hh}^2/S}^1 \frac{dx_1}{x_1} f_{g/p} \left( \frac{m_{hh}^2}{x_1 S}, \mu_f \right) \\ &\quad \times f_{g/p}(x_1, \mu_f) \int d\eta \left| \frac{\partial \hat{\eta}}{\partial \eta} \right|_{m_{hh}, \eta, x_1} \\ &\equiv \frac{m_{hh}}{S^2} \mathcal{H}(m_{hh}, \mu_r) \Sigma(m_{hh}, S, \mu_f). \end{aligned} \quad (9)$$

where  $\eta$  and  $\hat{\eta}$  is the rapidity of one of the Higgs bosons in the laboratory frame and center of mass (c.m.) frame, respectively.  $\sqrt{S}$  is the collision energy of the hadron collider,  $\mathcal{H}(m_{hh}, \mu_r)$  is the hard scattering cross section with  $\mu_r$  the renormalization scale,  $f_{g/p}$  is the gluon PDF with  $\mu_f$  the factorization scale. As argued above, the

cut efficiency depends on the configuration of the Higgs bosons which is described by  $m_{hh}$  and  $\eta$ , and the differential cross section after cuts is

$$\begin{aligned} \frac{d\sigma_{\text{cut}}}{dm_{hh}} &= \int d\tilde{m}_{hh} \frac{\tilde{m}_{hh}}{S^2} \mathcal{H}(\tilde{m}_{hh}, \mu_r) \int_{\tilde{m}_{hh}^2/S}^1 \frac{dx_1}{x_1} \\ &\quad \times f_{g/p} \left( \frac{\tilde{m}_{hh}^2}{x_1 S}, \mu_f \right) f_{g/p}(x_1, \mu_f) \int d\eta \\ &\quad \times \left| \frac{\partial \hat{\eta}}{\partial \eta} \right|_{\tilde{m}_{hh}, \eta, x_1} \epsilon(m_{hh}, \tilde{m}_{hh}, x_1, \eta), \end{aligned} \quad (10)$$

where  $\tilde{m}_{hh}$  is introduced to describe the finite energy smearing effect and  $\epsilon$  stands for the cut acceptance. Define

$$\begin{aligned} \tilde{\Sigma}(\tilde{m}_{hh}, S, \mu_f) &\equiv \int dm_{hh} \int_{\tilde{m}_{hh}^2/S}^1 \frac{dx_1}{x_1} f_{g/p} \left( \frac{\tilde{m}_{hh}^2}{x_1 S}, \mu_f \right) \\ &\quad \times f_{g/p}(x_1, \mu_f) \int d\eta \left| \frac{\partial \hat{\eta}}{\partial \eta} \right|_{m_{hh}, \eta, x_1} \\ &\quad \times \epsilon(m_{hh}, \tilde{m}_{hh}, x_1, \eta), \end{aligned} \quad (11)$$

then

$$\sigma_{\text{cut}} = \int d\tilde{m}_{hh} \frac{\tilde{m}_{hh}}{S^2} \mathcal{H}(\tilde{m}_{hh}, \mu_r) \tilde{\Sigma}(\tilde{m}_{hh}, S, \mu_f). \quad (12)$$

We introduce a differential cut efficiency function

$$\mathcal{A}(m_{hh}, S, \mu_f) = \frac{\tilde{\Sigma}(m_{hh}, S, \mu_f)}{\Sigma(m_{hh}, S, \mu_f)} \equiv \mathcal{A}(m_{hh}), \quad (13)$$

which depends on  $\sqrt{S}$ , parton distribution functions and kinematic cuts. Again, we emphasize that the  $\mathcal{A}$ -function is model independent. If the  $gg \rightarrow hh$  scattering in NP models is also dominated by the  $s$ -wave scattering, its production rate after cuts is

$$\sigma_{\text{cut}} = \int dm_{hh} \frac{d\sigma}{dm_{hh}} \otimes \mathcal{A}(m_{hh}, S, \mu_f). \quad (14)$$

The  $\mathcal{A}$ -function could be derived analytically for a given  $m_{hh}$ . It is hard to account for the detector effects analytically, however. In this work we first obtain the cut efficiency of signal events from the Monte Carlo simulation with all the detector effects and then fit the efficiency with the following functions as suggested by analytical calculations:

$$\mathcal{A}(m_{hh}) = \begin{cases} c_1 \left[ 1 - \sqrt{\frac{m_{hh}^2 (1 - \cos \Delta R_0) - 8(m_h - \delta m_1)^2}{(1 - \cos \Delta R_0)(m_{hh}^2 - 4(m_h - \delta m_1)^2)}} \right]^{\gamma_c}, & m_{hh} > m_{hh}^{(t)}, \\ c_2 \left[ 1 - \frac{4p_{T,h}^2}{m_{hh}^2 - 4(m_h - \delta m_2)^2} \right]^{\beta_a} \left( \frac{m_{hh}}{\sqrt{S}} \right)^{\beta_b} \left[ 1 + \beta_c \left( \frac{m_{hh}}{\sqrt{S}} \right) \log \left( \frac{2m_{hh}}{\sqrt{S}} \right) \right], & 329.3 \text{GeV} < m_{hh} < m_{hh}^{(t)}, \\ 0, & m_{hh} < 329.3 \text{GeV}. \end{cases} \quad (15)$$

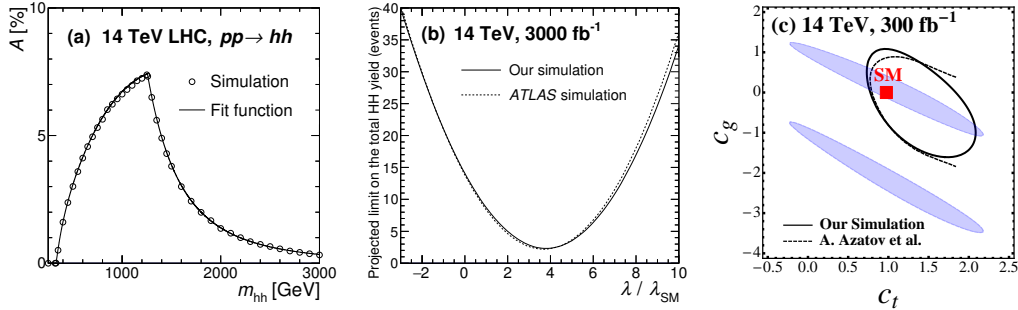


FIG. 4. (a): Cut efficiency as a function of  $m_{hh}$  at the 14TeV LHC; (b): comparison between our method (solid curve) and the ATLAS simulation (dashed line, see Fig. 8 in [72]); (c) comparison of 68% C.L. exclusion contours in the plane of  $c_g$  and  $c_t$  obtained in our method (solid curve) and the one in [4] (dashed curve) for the choice (b), i.e.  $c_{2h} = 3(c_t - 1)/2$ .

The  $\gamma_c$ ,  $\beta_{a,b,c}$  and  $\delta m_{1,2}$  parameters reflect the imperfect detector effects,  $c_{1,2}$  are the normalization parameters and  $m_{hh}^{(t)}$  is the turning point of two fitting functions.

Figure 4(a) displays the cut efficiency as a function of  $m_{hh}$  from the Monte Carlo simulation result (circle). We note that the efficiency depends mainly on the cut on  $p_T^{b\bar{b},\gamma\gamma}$  and  $\Delta R$ . The large  $p_T^{b\bar{b},\gamma\gamma}$  cuts require the Higgs boson's energy must be more than  $\sqrt{m_h^2 + p_T^2} \sim 167$  GeV such that  $m_{hh} > 330$  GeV. Therefore, the cut efficiency is zero for  $m_{hh} < 330$  GeV. The efficiency increases with  $m_{hh}$  because the  $p_T$ 's of Higgs boson decay products also increase with  $m_{hh}$  such that more signal events pass the  $p_T$  cuts. On the other hand,  $\Delta R_{b\bar{b}}$  decreases with  $m_{hh}^{(t)}$  and reaches  $\Delta R_0 = 0.4$  at  $m_{hh} = m_{hh}^{(t)}$ . For  $m_{hh} > m_{hh}^{(t)}$  the cut efficiency decreases with  $m_{hh}$  because  $\Delta R_{b\bar{b}}$  is likely to be smaller than 0.4 such that most of the signal events fail the  $\Delta R$  cut. We fit the Monte Carlo data with the  $\mathcal{A}$ -function in Eq. 15 and obtain those fitting parameters which are shown in Table I. We note that the fitting parameters are not sensitive to the PDF sets. Both CT14 and MSTW2008 PDF sets yield similar parameters. For comparison we also plot the fitting function in Fig. 4(a); see the solid curve.

TABLE I. Fitting parameters (the second and fifth rows) of  $\mathcal{A}(m_{hh})$  and the corresponding uncertainties (the third and sixth rows) for two PDF sets: (top) CT14 [74] and (bottom) MSTW2008 [75].

$m_{hh,0}$	$c_1$	$m_1$	$\gamma_c$	$c_2$	$\delta m_2$	$\beta_a$	$\beta_b$	$\beta_c$
1.257TeV	1.1378	50GeV	1.675	11.02	2.5GeV	1.13	1.48	4.88
–	0.0037	–	0.002	1.20	–	0.02	0.02	0.03
$m_{hh,0}$	$c_1$	$m_1$	$\gamma_c$	$c_2$	$\delta m_2$	$\beta_a$	$\beta_b$	$\beta_c$
1.254TeV	1.1419	50GeV	1.677	9.66	2.5GeV	1.13	1.44	4.82
–	0.0040	–	0.002	1.09	–	0.02	0.02	0.03

In order to check our method, we compare our results with those of the ATLAS collaboration [72] and Ref. [4]. The comparisons are shown in Fig. 4(b) and Fig. 4(c), respectively. Our results are consistent with those results in [4, 72]. Figure 4(c) shows the exclusion contours at 68% C.L. with  $\mathcal{L} = 300 \text{ fb}^{-1}$  for the case (b) of anomalous couplings.

**Conclusion and Discussion:** Now equipped with the cut efficiency function  $\mathcal{A}(m_{hh})$ , we are ready to estimate the potential of excluding the FNNP band at the LHC. The SM backgrounds include  $b\bar{b}\gamma\gamma$ ,  $cc\gamma\gamma$ ,  $b\bar{b}\gamma j$ ,  $jj\gamma\gamma$ ,  $b\bar{b}jj$ ,  $t\bar{t}(\geq 1\ell^\pm)$ ,  $t\bar{t}\gamma$ ,  $Z(\rightarrow b\bar{b})h(\rightarrow \gamma\gamma)$ ,  $t\bar{t}h(\rightarrow \gamma\gamma)$  and  $b\bar{b}h(\rightarrow \gamma\gamma)$ , etc. There are 4.72 background events after all the cuts at the 14 TeV LHC with an integrated luminosity of  $300 \text{ fb}^{-1}$  [72]. We calculate the 95% C.L. exclusion bound with

$$\sqrt{-2 \left( n_b \ln \frac{n_s + n_b}{n_b} - n_s \right)} = 1.96, \quad (16)$$

where  $n_s$  and  $n_b$  denotes the number of signal and background events, respectively.

Figure 5 displays the contours of 95% C.L. exclusion bound from the Higgs boson pair production with  $\mathcal{L} = 100 \text{ fb}^{-1}$  and  $300 \text{ fb}^{-1}$  at the 14 TeV LHC for the four choices of anomalous couplings. The exclusion contours of the cases (a) and (b) are different from those  $R_{hh}$  contours shown in Fig. 2. The differences occur in the large positive  $c_t$  region where  $\text{BR}(h \rightarrow \gamma\gamma)$  is highly reduced. A large  $c_g$  is needed to reach the same rate of the Higgs boson pair production.

In the case (c) the shapes of the exclusion bounds are very similar to those of the  $R_{hh}$  contours; see Fig. 5(c) and Fig. 2(c). It can be understood from the fact that the  $c_{2h}$  is not sensitive to the kinematic cuts or  $\text{Br}(h \rightarrow \gamma\gamma)$ .

In the case (d), the shape of exclusion bounds in Fig. 5(d) is slightly different from that of the  $R_{hh}$  contours in Fig. 2(d), especially in the small  $c_3$  region. The difference can be understood from the cuts we imposed.

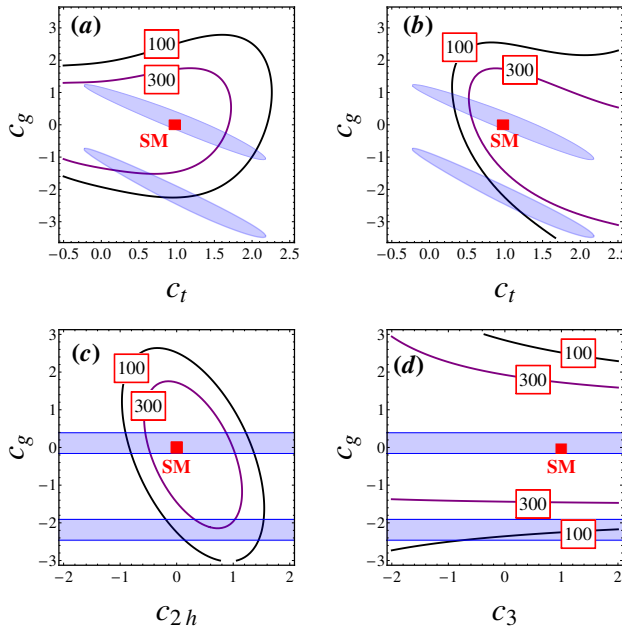


FIG. 5. The 95% C.L. exclusion contours in the plane of anomalous couplings obtained from the Higgs boson pair production with luminosity  $\mathcal{L} = 100 \text{ fb}^{-1}$  and  $300 \text{ fb}^{-1}$  at the 14 TeV LHC. The figure indices correspond to the benchmark choices of anomalous couplings in Eq. 5.

The  $c_3$  coupling contributes sizeably in the small  $m_{hh}$  region. However, the hard  $p_T$  cut on  $b\bar{b}$  and  $\gamma\gamma$  pairs demands a large  $m_{hh}$  region. As a result, the exclusion contours depend mildly on  $c_3$ . It is consistent with Ref. [68].

If no excess were observed in the Higgs boson pair production, then one can impose constraints on the anomalous couplings, especially on the FNNP band. The minimal luminosities to exclude the FNNP band at 95% C.L. in the four choices of anomalous couplings are

$$(a) : \mathcal{L} \geq 1681 \text{ fb}^{-1}; \quad (b) : \mathcal{L} \geq 235 \text{ fb}^{-1}; \\ (c) : \mathcal{L} \geq 446 \text{ fb}^{-1}; \quad (d) : \mathcal{L} \geq 186 \text{ fb}^{-1}.$$

It is worth mentioning that the current allowed bands shown in Fig. 1 would shrink when the LHC Run-2 data comes out. It is possible to exclude the FNNP band with a luminosity smaller than the values shown above.

*Note:* While this article was in finalization, the paper by B. Batell *et al* [78] appeared online and investigated the correlation between single Higgs and double Higgs boson production in supersymmetric model.

**Acknowledgments:** The work of QHC, BY and DMZ is supported in part by the National Science Foundation of China under Grand No. 11275009. HZ is supported by the U.S. DOE under contract No. DE-SC0011702. Part of this work was done while HZ was visiting the Center for High Energy Physics at Peking University. HZ is

pleased to recognize this support and the hospitality of the Center of HEP at Peking University.

\* qinghongcao@pku.edu.cn

† binyan@pku.edu.cn

‡ zhangdongming@pku.edu.cn

§ zhanghao@physics.ucsb.edu

- [1] G. Aad *et al.* (ATLAS) (2015), arXiv:1507.04548.
- [2] V. Khachatryan *et al.* (CMS), Eur. Phys. J. **C75**, 212 (2015), arXiv:1412.8662.
- [3] W.-F. Chang, W.-P. Pan, and F. Xu, Phys. Rev. **D88**, 033004 (2013), arXiv:1303.7035.
- [4] A. Azatov, R. Contino, G. Panico, and M. Son, Phys. Rev. **D92**, 035001 (2015), arXiv:1502.00539.
- [5] Q.-H. Cao, Talk given at the 13th Workshop on Heavy Flavor and CP Violation, Lanzhou, China, July 25, 2015, <http://indico.ihep.ac.cn/event/4774/session/6/contribution/15/material/slides/0.pdf>.
- [6] E. W. N. Glover and J. J. van der Bij, Nucl. Phys. **B309**, 282 (1988).
- [7] U. Baur, T. Plehn, and D. L. Rainwater, Phys. Rev. Lett. **89**, 151801 (2002), hep-ph/0206024.
- [8] U. Baur, T. Plehn, and D. L. Rainwater, Phys. Rev. **D67**, 033003 (2003), hep-ph/0211224.
- [9] M. J. Dolan, C. Englert, and M. Spannowsky, JHEP **1210**, 112 (2012), arXiv:1206.5001.
- [10] A. Papaefstathiou, L. L. Yang, and J. Zurita, Phys. Rev. **D87**, 011301 (2013), arXiv:1209.1489.
- [11] J. Baglio, A. Djouadi, R. Grber, M. Mhleitner, J. Quevillon, *et al.*, JHEP **1304**, 151 (2013), arXiv:1212.5581.
- [12] F. Goertz, A. Papaefstathiou, L. L. Yang, and J. Zurita, JHEP **1306**, 016 (2013), arXiv:1301.3492.
- [13] A. J. Barr, M. J. Dolan, C. Englert, and M. Spannowsky, Phys. Lett. **B728**, 308 (2014), arXiv:1309.6318.
- [14] V. Barger, L. L. Everett, C. Jackson, and G. Shaughnessy, Phys. Lett. **B728**, 433 (2014), arXiv:1311.2931.
- [15] Q. Li, Q.-S. Yan, and X. Zhao, Phys. Rev. **D89**, 033015 (2014), arXiv:1312.3830.
- [16] D. E. Ferreira de Lima, A. Papaefstathiou, and M. Spannowsky, JHEP **1408**, 030 (2014), arXiv:1404.7139.
- [17] M. Slawinska, W. van den Wollenberg, B. van Eijk, and S. Bentvelsen (2014), arXiv:1408.5010.
- [18] C. Englert, F. Krauss, M. Spannowsky, and J. Thompson, Phys. Lett. **B743**, 93 (2015), arXiv:1409.8074.
- [19] T. Liu and H. Zhang (2014), arXiv:1410.1855.
- [20] A. J. Barr, M. J. Dolan, C. Englert, D. E. Ferreira de Lima, and M. Spannowsky, JHEP **1502**, 016 (2015), arXiv:1412.7154.
- [21] Q. Li, Z. Li, Q.-S. Yan, and X. Zhao, Phys. Rev. **D92**, 014015 (2015), arXiv:1503.07611.
- [22] A. Papaefstathiou (2015), arXiv:1504.04621.
- [23] H.-J. He, J. Ren, and W. Yao (2015), arXiv:1506.03302.
- [24] T. Plehn, M. Spira, and P. Zerwas, Nucl. Phys. **B479**, 46 (1996), hep-ph/9603205.
- [25] A. Djouadi, W. Kilian, M. Muhleitner, and P. Zerwas, Eur. Phys. J. **C10**, 45 (1999), hep-ph/9904287.
- [26] A. Belyaev, M. Drees, O. J. Eboli, J. Mizukoshi, and S. Novaes, Phys. Rev. **D60**, 075008 (1999), hep-ph/9905266.
- [27] A. Belyaev, M. Drees, and J. Mizukoshi, Eur. Phys. J.

**C17**, 337 (2000), hep-ph/9909386.

[28] A. Belyaev, M. Drees, O. J. Eboli, J. Mizukoshi, and S. Novaes, pp. 748–751 (1999), hep-ph/9910400.

[29] R. Lafaye, D. Miller, M. Muhlleitner, and S. Moretti (2000), hep-ph/0002238.

[30] A. Barrientos Bendezu and B. A. Kniehl, Phys.Rev. **D64**, 035006 (2001), hep-ph/0103018.

[31] U. Baur, T. Plehn, and D. L. Rainwater, Phys.Rev. **D68**, 033001 (2003), hep-ph/0304015.

[32] U. Baur, T. Plehn, and D. L. Rainwater, Phys.Rev. **D69**, 053004 (2004), hep-ph/0310056.

[33] J.-J. Liu, W.-G. Ma, G. Li, R.-Y. Zhang, and H.-S. Hou, Phys.Rev. **D70**, 015001 (2004), hep-ph/0404171.

[34] M. Moretti, S. Moretti, F. Piccinini, R. Pittau, and A. Polosa, JHEP **0502**, 024 (2005), hep-ph/0410334.

[35] T. Binoth, S. Karg, N. Kauer, and R. Ruckl, Phys.Rev. **D74**, 113008 (2006), hep-ph/0608057.

[36] H. de Sandes and R. Rosenfeld, Phys.Lett. **B659**, 323 (2008), arXiv:0706.2665.

[37] L. Wang and J. M. Yang, Phys.Rev. **D77**, 015020 (2008), arXiv:0710.5038.

[38] W. Ma, C.-X. Yue, and Y.-Z. Wang, Phys.Rev. **D79**, 095010 (2009), arXiv:0905.0597.

[39] A. Arhrib, R. Benbrik, C.-H. Chen, R. Guedes, and R. Santos, JHEP **0908**, 035 (2009), arXiv:0906.0387.

[40] X.-F. Han, L. Wang, and J. M. Yang, Nucl.Phys. **B825**, 222 (2010), arXiv:0908.1827.

[41] E. Asakawa, D. Harada, S. Kanemura, Y. Okada, and K. Tsumura, Phys.Rev. **D82**, 115002 (2010), arXiv:1009.4670.

[42] R. Grober and M. Muhlleitner, JHEP **1106**, 020 (2011), arXiv:1012.1562.

[43] T. Figy and R. Zwicky, JHEP **1110**, 145 (2011), arXiv:1108.3765.

[44] M. Gillioz, R. Grober, C. Grojean, M. Muhlleitner, and E. Salvioni, JHEP **1210**, 004 (2012), arXiv:1206.7120.

[45] G. D. Kribs and A. Martin, Phys.Rev. **D86**, 095023 (2012), arXiv:1207.4496.

[46] S. Dawson, E. Furlan, and I. Lewis, Phys.Rev. **D87**, 014007 (2013), arXiv:1210.6663.

[47] M. J. Dolan, C. Englert, and M. Spannowsky, Phys.Rev. **D87**, 055002 (2013), arXiv:1210.8166.

[48] J. Cao, Z. Heng, L. Shang, P. Wan, and J. M. Yang, JHEP **1304**, 134 (2013), arXiv:1301.6437.

[49] D. T. Nhungh, M. Muhlleitner, J. Streicher, and K. Walz, JHEP **1311**, 181 (2013), arXiv:1306.3926.

[50] U. Ellwanger, JHEP **1308**, 077 (2013), arXiv:1306.5541.

[51] K. Nishiwaki, S. Niyogi, and A. Shivaji, JHEP **1404**, 011 (2014), arXiv:1309.6907.

[52] N. Haba, K. Kaneta, Y. Mimura, and E. Tsedenbaljir, Phys.Rev. **D89**, 015018 (2014), arXiv:1311.0067.

[53] T. Enkhbat, JHEP **1401**, 158 (2014), arXiv:1311.4445.

[54] J. Liu, X.-P. Wang, and S.-h. Zhu (2013), arXiv: 1310.3634.

[55] N. Kumar and S. P. Martin, Phys.Rev. **D90**, 055007 (2014), arXiv:1404.0996.

[56] W. Xiao-ping and Z. Shou-hua (2014), arXiv:1405.1800.

[57] C.-R. Chen and I. Low, Phys.Rev. **D90**, 013018 (2014), arXiv:1405.7040.

[58] C.-Y. Chen, S. Dawson, and I. Lewis, Phys.Rev. **D90**, 035016 (2014), arXiv:1406.3349.

[59] A. Ahriche, A. Arhrib, and S. Nasri, Phys.Lett. **B743**, 279 (2015), arXiv:1407.5283.

[60] V. Barger, L. L. Everett, C. Jackson, A. D. Peterson, and G. Shaughnessy, Phys.Rev.Lett. **114**, 011801 (2015), arXiv:1408.0003.

[61] V. Barger, L. L. Everett, C. B. Jackson, A. D. Peterson, and G. Shaughnessy, Phys.Rev. **D90**, 095006 (2014), arXiv:1408.2525.

[62] J. Cao, D. Li, L. Shang, P. Wu, and Y. Zhang, JHEP **1412**, 026 (2014), arXiv:1409.8431.

[63] S. Dawson, A. Ismail, and I. Low (2015), arXiv:1504.05596.

[64] T. Enkhbat (2015), arXiv:1504.08305.

[65] S. M. Etesami and M. M. Najafabadi (2015), arXiv:1505.01028.

[66] A. Pierce, J. Thaler, and L.-T. Wang, JHEP **05**, 070 (2007), hep-ph/0609049.

[67] S. Kanemura and K. Tsumura, Eur. Phys. J. **C63**, 11 (2009), arXiv:0810.0433.

[68] R. Contino, M. Ghezzi, M. Moretti, G. Panico, F. Piccinini, et al., JHEP **1208**, 154 (2012), arXiv:1205.5444.

[69] F. Goertz, A. Papaefstathiou, L. L. Yang, and J. Zurita, JHEP **1504**, 167 (2015), arXiv:1410.3471.

[70] L. Edelhaeuser, A. Knochel, and T. Steeger (2015), arXiv:1503.05078.

[71] C.-T. Lu, J. Chang, K. Cheung, and J. S. Lee (2015), arXiv:1505.00957.

[72] ATLAS Collaboration, Tech. Rep. ATL-PHYS-PUB-2014-019, CERN, Geneva (2014).

[73] J. Alwall, R. Frederix, S. Frixione, V. Hirschi, F. Maltoni, et al., JHEP **1407**, 079 (2014), arXiv:1405.0301.

[74] S. Dulat, T. J. Hou, J. Gao, M. Guzzi, J. Huston, P. Nadolsky, J. Pumplin, C. Schmidt, D. Stump, and C. P. Yuan (2015), arXiv:1506.07443.

[75] A. D. Martin, W. J. Stirling, R. S. Thorne, and G. Watt, Eur. Phys. J. **C63**, 189 (2009), 0901.0002.

[76] ATLAS Collaboration, Tech. Rep. ATL-PHYS-PUB-2013-004, CERN, Geneva (2013).

[77] ATLAS Collaboration, Tech. Rep. ATL-PHYS-PUB-2013-009, CERN, Geneva (2013).

[78] B. Batell, M. McCullough, D. Stolarski, and C. B. Verhaaren (2015), arXiv:1508.01208.